RDE Restorative Dentistry & Endodontics

Research Article

eISSN 2234-7666
Restor Dent Endod. 2026 May;51(2):e20
https://doi.org/10.5395/rde.2026.51.e20

Initial attachment, viability, proliferation, and migration of osteoblast-like SaOS-2 cells on two resorbable xenogeneic membranes for guided tissue regeneration: an *in vitro* experimental study

Rafael Fernández-Grisales[1,*], Giovanna García-Suárez[2], Ximena Guerrero-Rodríguez[2], Carolina Berruecos-Orozco[1], Marco Calle-Jaramillo[1], Wilder Javier Rojas[1], Vanessa Esmeralda Duque[1], Daniela Serna-Guisao[1], Néstor Ríos-Osorio[1,3]

[1]Department of Endodontics, CES University, Medellin, Colombia
[2]Department of Endodontics, Institución Universitaria Colegios de Colombia UNICOC, Bogotá, Colombia
[3]PhD Program Biomedical Sciences, Universidad el Bosque, Bogotá, Colombia

ABSTRACT

Objectives: This study evaluated the biocompatibility of a new xenogeneic resorbable membrane derived from porcine esophagus membrane (Quirumatrix, Cells Tech Co.) and compared it with a porcine pericardium membrane (Straumann Jason, Straumann Holding AG.) traditionally used for guided tissue regeneration. The parameters investigated were the viability, migration, and adhesion of SaOS-2 osteoblast-like cells derived from osteosarcoma on both membranes.

Methods: The cells were cultured in 100 mm plates in RPMI 1640 medium (40 mL), supplemented. They were incubated at 37°C in a humidified atmosphere with 95% air and 5% to 10% CO_2. Cell morphology and adhesion were evaluated using phase contrast optical microscopy and scanning electron microscope. Cell viability and proliferation were evaluated using a fluorometric resazurin reduction assay, with fluorescence intensity measured at 48, 72, and 96 hours. Cell migration was evaluated using staining with Alexa Fluor 555 Phalloidin (Cell Signaling Technology) and DAPI, with a reference line. Cell migration was analyzed by measuring displacement within the delineated area using an Axio Imager M2 fluorescence microscope (Carl Zeiss). Each membrane was photographed. The statistical analysis was performed using GraphPad Prism ver. 10.2.3 (GraphPad Software). A p-value <0.05 was considered significant between experimental groups.

Results: Both membranes were shown to be biocompatible. The porcine pericardium membrane showed greater cell adhesion and proliferation compared to the porcine esophagus membrane. Cell migration was significantly greater in the Jason membrane.

Conclusions: The results revealed that both evaluated membranes are biocompatible and non-cytotoxic; further research is needed to understand their long-term behavior, interactions with other types of cells, and performance in specific therapeutic situations.

Keywords: Biocompatibility; Cell migration; Cell proliferation; Cell viability; Guided tissue regeneration

Received: July 15, 2025 **Revised:** December 29, 2025 **Accepted:** January 2, 2026

Citation
Fernández-Grisales R, García-Suarez G, Guerrero-Rodríguez X, Berruecos-Orozco C, Calle-Jaramillo M, Rojas WJ, Duque VE, Serna-Guisao D, Ríos-Osorio N. Initial attachment, viability, proliferation and migration of osteoblast-like SaOS-2 cells on two resorbable xenogeneic membranes for guided tissue regeneration: an *in vitro* experimental study. Restor Dent Endod 2026;51(2):e20.

***Correspondence to**
Rafael Fernández-Grisales, DDS, MSc
Department of Endodontics, CES University, Calle 10A #22-04, Medellin, Colombia
Email: rfernandez@ces.edu.co

© 2026 The Korean Academy of Conservative Dentistry

This is an Open Access article distributed under the terms of the Creative Commons Attribution Non-Commercial License (https://creativecommons.org/licenses/by-nc/4.0/) which permits unrestricted non-commercial use, distribution, and reproduction in any medium, provided the original work is properly cited.

INTRODUCTION

Endodontic surgery is indicated for teeth presenting with persistent apical periodontitis (AP) in which non-surgical root canal treatment has failed or is not feasible [1]. The initiation and progression of AP result from a dynamic interplay between persistent antigenic stimuli—primarily toxins and bacterial by-products originating from an infected root canal system—and the host immune response [2]. Consequently, the principal objective of endodontic surgery is to eliminate or effectively isolate the source of infection, thereby creating biological conditions conducive to periapical tissue healing [1,2].

Histological outcomes of periapical healing following successful endodontic surgery may be categorized as repair or regeneration, depending on lesion characteristics, the availability of resident stem/progenitor cells and growth factors, and the local microenvironmental cues at the surgical site [1,3]. Regeneration entails the reconstitution of periapical tissues—namely bone, periodontal ligament, and root cementum—thereby restoring native architecture and function, whereas repair represents a non-specific healing response characterized by fibrosis and scar formation. Healing by repair frequently fails to restore full tissue function and may result in residual structural irregularities at the injury site [1,3]. Although regeneration constitutes the preferred surgical outcome, its attainment remains challenging, as it is critically dependent on the cellular, molecular, and behavioral properties of periapical tissues throughout the healing cascade [4,5].

Periapical sites—particularly large endodontic lesions—managed by conventional endodontic surgery are frequently repopulated by fibrous connective tissue, a histological correlate of incomplete periapical healing [5]. The ingrowth of non-osteogenic tissues into the post-surgical osseous defect, together with epithelial down-growth along the root surface, may bias healing towards repair rather than true regeneration [4,5]. Accordingly, if colonization of the defect by gingival connective tissue or oral epithelium can be sufficiently delayed to permit the establishment of cells with regenerative capacity—most notably periodontal ligament- and bone-derived cells, epithelial migration may be restrained, and regenerative healing facilitated [4–6].

Currently, there is growing interest in the application of guided tissue regeneration (GTR) strategies as adjuncts to endodontic surgery, incorporating bone grafts and barrier membranes to modulate the local microenvironment in favor of tissue and bone regeneration within periapical defects [1,7]. Notably, a recent systematic review and meta-analysis demonstrated that regenerative protocols employing collagen membranes in combination with bovine-derived hydroxyapatite significantly enhance periapical lesion healing following endodontic surgery [1].

Barrier membranes are designed to inhibit the apical migration of epithelial cells into the surgical defect. An ideal membrane should combine ease of handling with bioabsorbability and biofunctionality [1,8]. Nevertheless, currently available resorbable membranes often fail to achieve complete periapical tissue regeneration, largely due to inflammatory responses arising from insufficient microenvironmental isolation [8]. Consequently, the use of high-biocompatibility barrier membranes is critical for optimizing GTR outcomes and overcoming these limitations [8]. In addition, barrier membranes should support cell adhesion and progenitor cell migration [9]. Osteoblastic progenitor cells must adhere to an appropriate substrate before initiating the wound-healing cascade, including proliferation, differentiation, and subsequent tissue maturation. This attachment process proceeds through four sequential stages: (i) adsorption of glycoproteins onto the substrate surface, (ii) initial cell contact, (iii) stable attachment, and (iv) cell spreading, after which cellular replication is initiated [9]. Despite this, the influence of barrier membrane composition on osteoblastic attachment and behavior remains incompletely understood.

In light of the foregoing, the present *in vitro* study was designed to investigate the biocompatibility of two commercially available xenogeneic resorbable barrier membranes—Straumann Jason (Straumann Holding AG., Basel, Switzerland) and Quirumatrix (Cells Tech Co., Medellín, Colombia)—derived from native collagen and extracellular matrix (ECM), respectively. Specifically, the study sought to provide a comparative biological appraisal by evaluating: (i) the ability of osteoblast-like SaOS-2 cells to adhere to each membrane, (ii) cell vi-

https://doi.org/10.5395/rde.2026.51.e20

ability and proliferative capacity following membrane contact, and (iii) the migratory behavior of SaOS-2 cells across the membrane surfaces.

METHODS

Membranes examined

Two commercially available GTR membranes were evaluated: Quirumatrix (an ECM-derived membrane obtained from decellularized porcine esophagus) and Straumann Jason (a native porcine collagen pericardium-derived membrane) (Figure 1).

Cell culture on barrier membranes

Osteosarcoma-derived Osteoblast-like cells, SaOS-2 (ATCC HTB-85) were purchased from American Type Culture Collection- ATCC Inc. (Manassas, VA, USA). Cells were cultivated in 100-mm culture dishes, ingrown in RPMI 1640 (40 mL) medium (Sigma-Aldrich R4130; Sigma-Aldrich, St. Louis, MO, USA) supplemented with fetal bovine serum (FBS; GE Healthcare Life Sciences, cat. #SH30088.03) and 1% penicillin-streptomycin-amphotericin B (HyClone, Logan, UT, USA; Ref. #SV30079.01). Cells were incubated at 37°C in a humidified atmosphere of 95% air, and 5%–10% CO_2. The medium was changed every 2 days.

First, we followed a standardization protocol to provide optimal conditions for cell attachment and viability assays for both barrier membranes. Initially, the hydration of the membranes was evaluated with DMEM/F12 (Biowest, Nuaillé, France; Ref. #L0090-500) medium, supplemented with different concentrations (10%, 20%) of FBS (GE Healthcare Life Sciences, cat. #SH30088.03) or 100% FBS, before cells were seeded. Better attachment and cell viability were observed on membranes with 100% FBS hydration for 48 hours prior to cell seeding (see cell attachment and viability below).

Once the most appropriate method of hydrating the

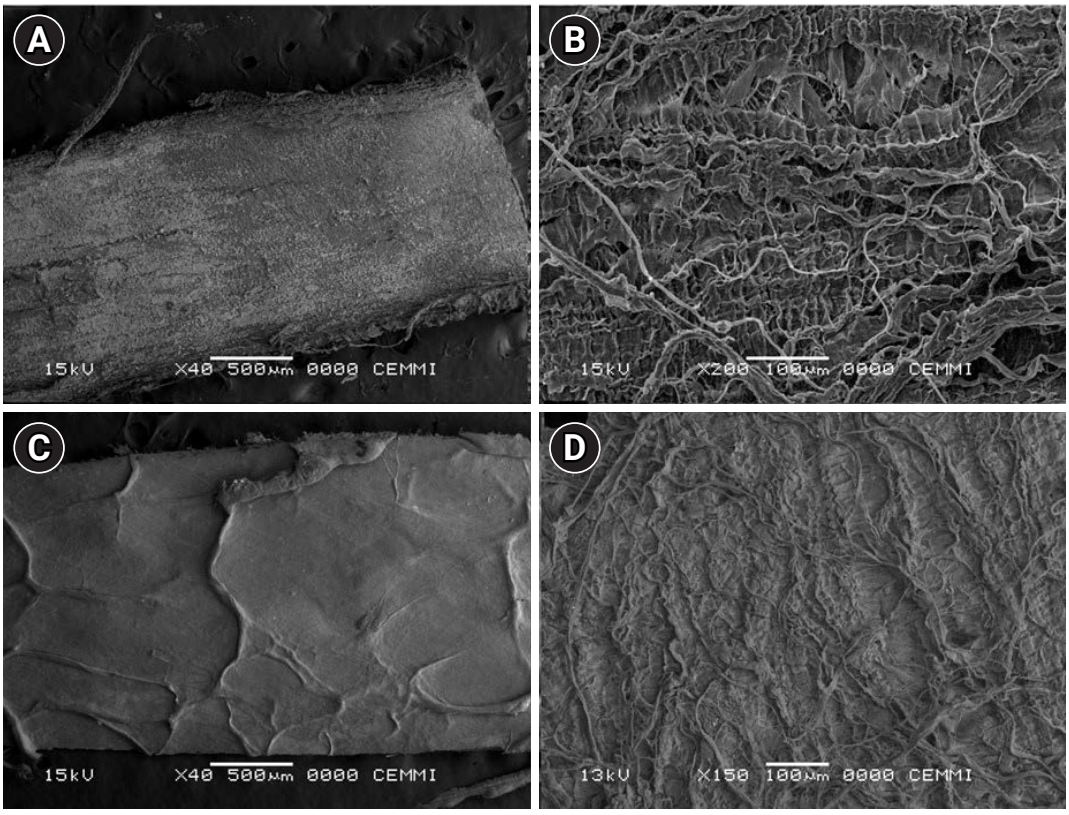


Figure 1. Surface morphology (structure and mesh) scanning electron micrographs of the examined bioabsorbable membranes. (A, B) Jason (Straumann Holding AG., Basel, Switzerland) and (C, D) Quirumatrix (Cells Tech Co., Medellín, Colombia). Magnification bar, 100 µm.

membranes was standardized to allow the maximum percentage of viability and cell attachment, membranes were cut into discs 5 × 3 mm in area, placed into 12-well culture plates with a polyvinyl chloride surgical tape (Micropore; 3M, St. Paul, MN, USA) and hydrated with 100% FBS (GE Healthcare Life Sciences, cat. #SH30088.03) for 48 hours before cell seeding. SaOS-2 cultured in 100-mm culture dishes were trypsinized (0.25% trypsin, SV30037.01, GE Healthcare Life Sciences), and 40,000 cells (in 1 mL of fresh medium) per well were seeded in triplicate onto the 12-well culture plates with or without membranes (control group/cells) (Figure 2).

Visualization of cell attachment and morphological changes

Morphological/phenotypic changes were monitored daily up to 5 days after cell seeding, using phase contrast-light microscopy (Zeiss Axio Imager M2 inverted microscope; Carl Zeiss, Jena, Germany) and compared to control cells (cells seeded directly into each well without a membrane).

Upon completion of a 5-day seeding period, barrier membranes (Jason and Quirumatrix) were prepared for examination under a scanning electron microscope (SEM) to evaluate cell morphology and attachment. Cells were fixed with 2.5% glutaraldehyde (Sigma-Aldrich) for 2 hours, then rinsed three times with phosphate-buffered saline (PBS, Ref. #158127; Sigma-Aldrich). Secondary fixation was carried out using 1% osmium tetroxide. Thereafter, the samples were dehydrated for 30 minutes using a graded series of ethanol (50%, 70%, 90%, and 100%) for 20 minutes each. The samples were subsequently sputtered (gold/palladium sputter-coated) and analyzed with Vega-TEScan (Tescan USA Inc., Warrendale, PA, USA) at an accelerating voltage of 20 kV.

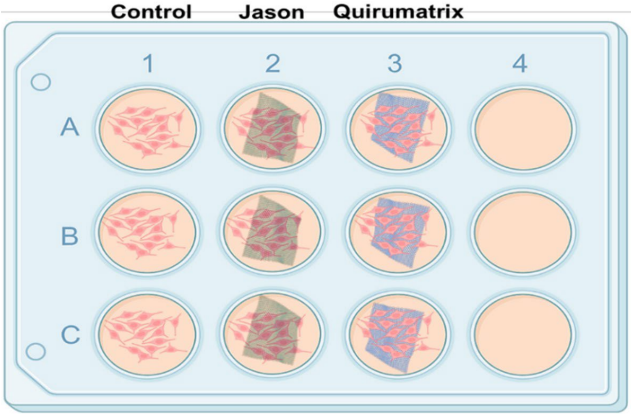


Figure 2. Both membranes (discs 5 × 3 mm in area) were prepared for cell culture. SaOS-2 cells (40,000 cells/mL) were seeded in triplicate into a new 12-well plate containing 1 mL of fresh medium per well. (A) Control group. B) Jason (Straumann Holding AG., Basel, Switzerland). (C) Quirumatrix (Cells Tech Co., Medellín, Colombia).

Representative SEM images were randomly selected from multiple fields of view, prioritizing those that displayed the most common cell morphologies and attachment patterns for each membrane type. Images with artefacts or atypical features were excluded to ensure accurate representation of the experimental findings.

Fluorometric resazurin reduction assay for cell viability

The viability and proliferation of SaOS-2 cells were assessed by fluorometric resazurin reduction assay. Briefly, Resazurin (7-hydroxy-3H-phenoxazin-3-one 10-oxide) is a non-fluorescent molecule that may infiltrate cells, be reduced to highly fluorescent resorufin in the intracellular space and detect changes in oxidation state using fluorometric techniques. This test allowed us to make conclusions on metabolic activity (mitochondrial activity), as the reducing environment can only be sustained with an active intermediate metabolism.

Cells seeded in multiwell plates were spiked with 4.4 µg/well of resazurin solution and incubated at 37°C for four hours. Thereafter, the fluorescence intensity was measured at 48, 72, and 96 hours, using a Tecan Infinite M2000 Pro reader (Tecan, Männedorf, Switzerland) at 535-595 nm wavelengths [10]. Each membrane was removed from the culture well to assess the fluorescence produced by cells adherent to the well versus those adherent to the membrane individually. After each fluorescence reading, each membrane was returned to its corresponding well until a new fluorescence reading was recorded. To evaluate whether the fluorescence measurement obtained by reduced resazurin was proportional to the number of live cells present, a correlation between the quantity of resorufin produced by known concentrations of SaOS-2 cells was established. Cells were serially diluted (80,000, 40,000, 20,000, and

https://doi.org/10.5395/rde.2026.51.e20

10,000). The fluorescence measurements showed that resorufin production was proportional to the number of viable cells. The linear regression analysis indicated a high correlation coefficient (R^2 = 0.993) within the 10,000–80,000 cell range (Figure 3).

Cell migration

The migration assay was performed as previously reported by Takata *et al.* [11]. Membranes were prepared and placed into 12-well culture plates as previously described. The membranes were hydrated with 100% FBS (GE Healthcare Life Sciences, Cat #SH30088.03) for 48 hours. Membranes were then washed with PBS (Sigma-Aldrich, Ref. #P4417). Half of each membrane was covered with sterile surgical tape (Micropore) (Figure 4A, B). A total of 40,000 osteoblast-like SaOS-2 cells were seeded on the non-covered half and allowed to attach for 24 hours. Thereafter, the wells were rinsed with PBS (Sigma-Aldrich, Ref. #P4417) and the surgical tape was removed to allow cell migration (for 3 days). The boundary between the covered and uncovered areas of barrier membranes was marked as a reference line for cell migration. Three days later, the membranes were fixed with 4% paraformaldehyde (Sigma-Aldrich, Ref. #158127) and stained with Alexa Fluor 555 Phalloidin (Cell Signaling Technology #8953) and 4′,6-diamidino-2-phenylindole (DAPI; Cell Signaling Technology). Phalloidin fluorescently stains the cell cytoskeleton through the binding of phalloidin to F-actin. DAPI allows the visualization of nuclear DNA in fixed cells. Having the reference line, cell migration was analyzed by measuring cell displacement through the delimited area. The number of cells was counted under an Axio Imager M2 fluorescence microscope. Each membrane was photographed with an AxioCam HR camera (Carl Zeiss). The visual field for cell counting was selected randomly (Figure 5).

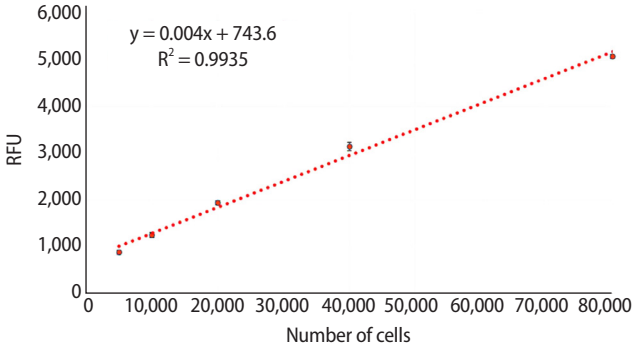


Figure 3. Calibration curve that shows the relationship between the number of SaOS-2 cells and resorufin synthesis via resazurin reduction. RFU, relative fluorescence unit.

Statistical analysis

All experiments were performed at least three times independently, with each condition analyzed in triplicate within each experiment, resulting in a total of nine independent measurements per condition (n = 9). Data

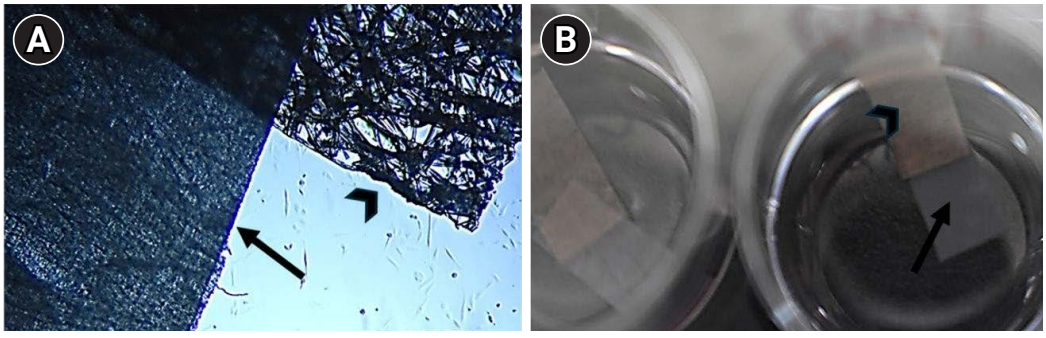


Figure 4. SaOS-2 cell migration assay on Jason (Straumann Holding AG., Basel, Switzerland) and Quirumatrix (Cells Tech Co., Medellín, Colombia) membranes. The membranes (arrow) were placed in 12-well plates with surgical tape (arrowhead), hydrated for 48 hours with 100% fetal bovine serum, and then washed with phosphate-buffered saline. Half of each membrane was covered with sterile surgical tape. 40,000 osteoblast-like SaOS-2 cells were seeded on the non-covered side and allowed to adhere for 24 hours before the surgical tape was removed, thus allowing cell migration. (A) A photomicrograph of the Jason membrane and surgical tape fixing under a microscope. (B) A photograph of the culture well, showing the membrane with a section covered in surgical tape.

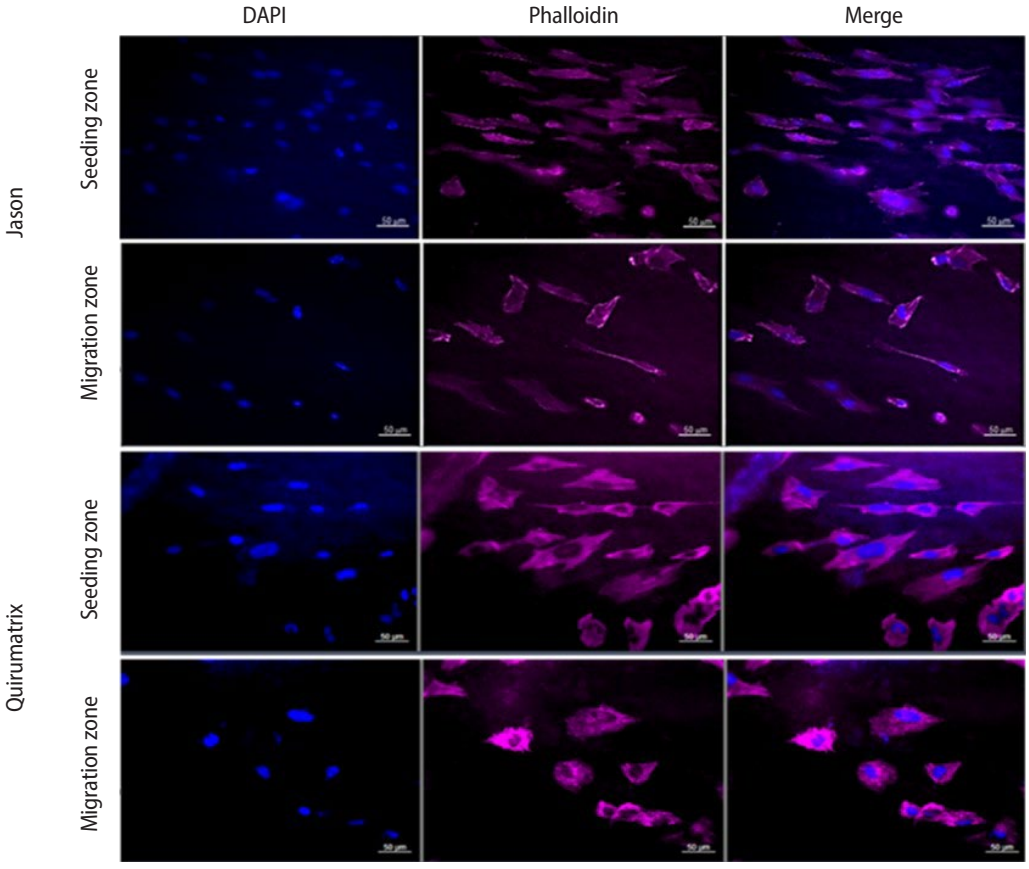


Figure 5. Staining of SaOS-2 cells with Alexa Fluor 555 Phalloidin (Cell Signaling Technology, Danvers, MA, USA) and 4′,6-diamidino-2-phenylindole (DAPI) on barrier membranes to evaluate cell migration. Staining was performed on nine membranes of each type, and cell counts were collected from 10 pictures of each membrane at 20× magnification. Magnification bar 50 µm. Jason: Straumann Holding AG., Basel, Switzerland; Quirumatrix: Cells Tech Co., Medellín, Colombia.

are presented as mean ± standard deviation. Prior to statistical comparison, data distributions were assessed for normality using the Shapiro-Wilk test and for homogeneity of variances using the Levene test. For datasets fulfilling parametric assumptions, comparisons between two experimental groups were performed using the Student *t*-test, whereas comparisons involving more than two groups were analyzed using one-way analysis of variance. When the data did not meet the assumptions of normality and/or homoscedasticity, the nonparametric Mann-Whitney *U* test was used for pairwise comparisons. A p-value <0.05 was considered statistically significant. All statistical analyses were conducted using GraphPad Prism (ver. 10.2.3; GraphPad Software, San Diego, CA, USA).

RESULTS

Visualization of cell attachment and morphological changes

Phase contrast-light microscopy did not provide any evidence of any influence from membrane hazardous residues or the glue from the double-sided adhesive tape throughout the first 5 days of the experiment after cell seeding. There was no interference with the proliferation of cells on the culture plates next to the barrier membranes and tape. There was no evidence of cell detachment or death. SEM examination after 5 days of cell seeding revealed a smaller number of cells attached to Quirumatrix membranes compared to cells on Jason membranes.

Under SEM examination, cells attached to the Jason

https://doi.org/10.5395/rde.2026.51.e20

membrane were elongated and star-shaped, whereas cells attached to the Quirumatrix membrane were more triangular. Furthermore, cells on Jason membranes were observed to emit protrusions from the cell membrane known as "Blebs" (Figures 6–8).

Cell proliferation

Values from the previously provided calibration curves (Figure 3) were used to calculate the number of cells for each fluorescence measurement: membrane, well, and total number of cells (well + membrane) at different times (48, 72, and 96 hours) (Figure 9A–C).

As shown in Figure 9A, the number of cells on the Jason membrane is significantly higher than that on the Quirumatrix membrane after 72 and 96 hours of seeding. Figure 9B indicates that the number of cells in the wells of the culture plate with the Jason membrane and the Quirumatrix is lower than in the wells without the membrane (control). The differences were significant ($p < 0.05$) at 96 hours following seeding.

At 96 hours, when the number of cells identified on the membranes was added up with the number of cells adhered to the corresponding well, it was shown that both Jason and Quirumatrix membranes had considerably more total cells than the control group ($p < 0.05$) (Figure 9C).

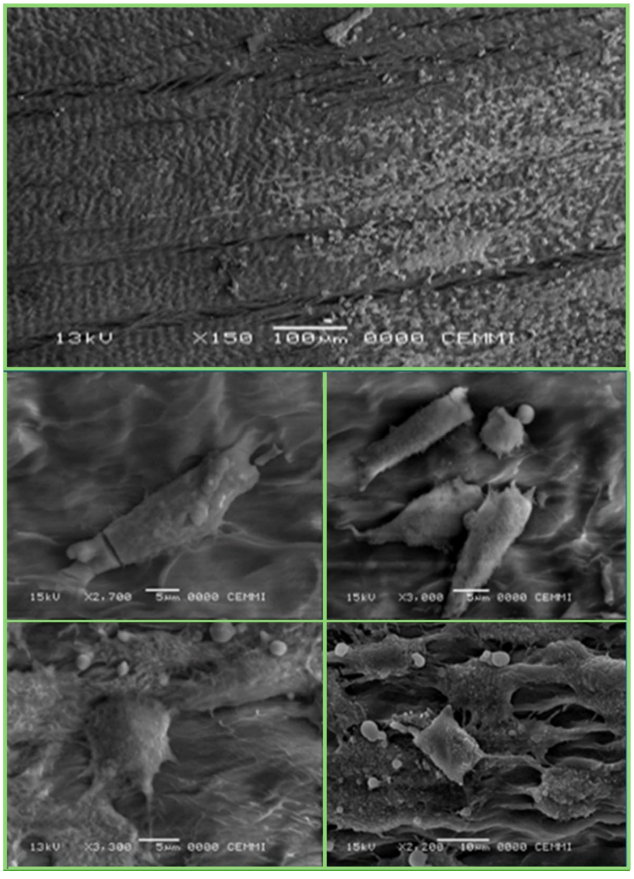


Figure 6. Scanning electron micrographs of SaOS-2 osteoblast-like cells attached to the surface of the Jason membrane (Straumann Holding AG., Basel, Switzerland). The cells have an expanded morphology, with many cytoplasmic extensions interacting directly with the membrane's collagen fibers.

Cell migration

After 3 days of culture, SaOS-2 cells adhered to the bottom of the culture plate and to the membranes; cell migration through the membranes was observed to different degrees (cell photographs) (Figure 9A–C). In the Jason membranes, more cells were observed in the migration zone than in the Quirumatrix membranes; this difference was statistically significant ($p < 0.05$). The seeding zone showed no significant differences between the two membranes (Figure 10).

DISCUSSION

This *in vitro* study evaluated the biocompatibility of two xenogeneic porcine-derived barrier membranes—a novel ECM-derived membrane obtained from decellularized porcine esophagus (Quirumatrix) and a native porcine pericardium collagen membrane (Straumann Jason)—by analyzing osteoblast-like SaOS-2 cell attachment, proliferation, migratory, and viability, behavior [1,9,11,12]. The selection of SaOS-2 osteoblast-like cells as the experimental model warrants consideration. While primary periodontal ligament cells or bone marrow-derived mesenchymal stem cells would more closely recapitulate the physiological regenerative environment, SaOS-2 cells offer distinct advantages for preliminary biocompatibility screening [13,14]. This cell line is well-characterized, exhibits key osteoblastic features including alkaline phosphatase activity and mineralization capacity, and has been extensively validated for evaluating cell–material interactions in biomaterial research [15]. Importantly, the use of a standardized cell line ensures reproducibility and eliminates donor-re-

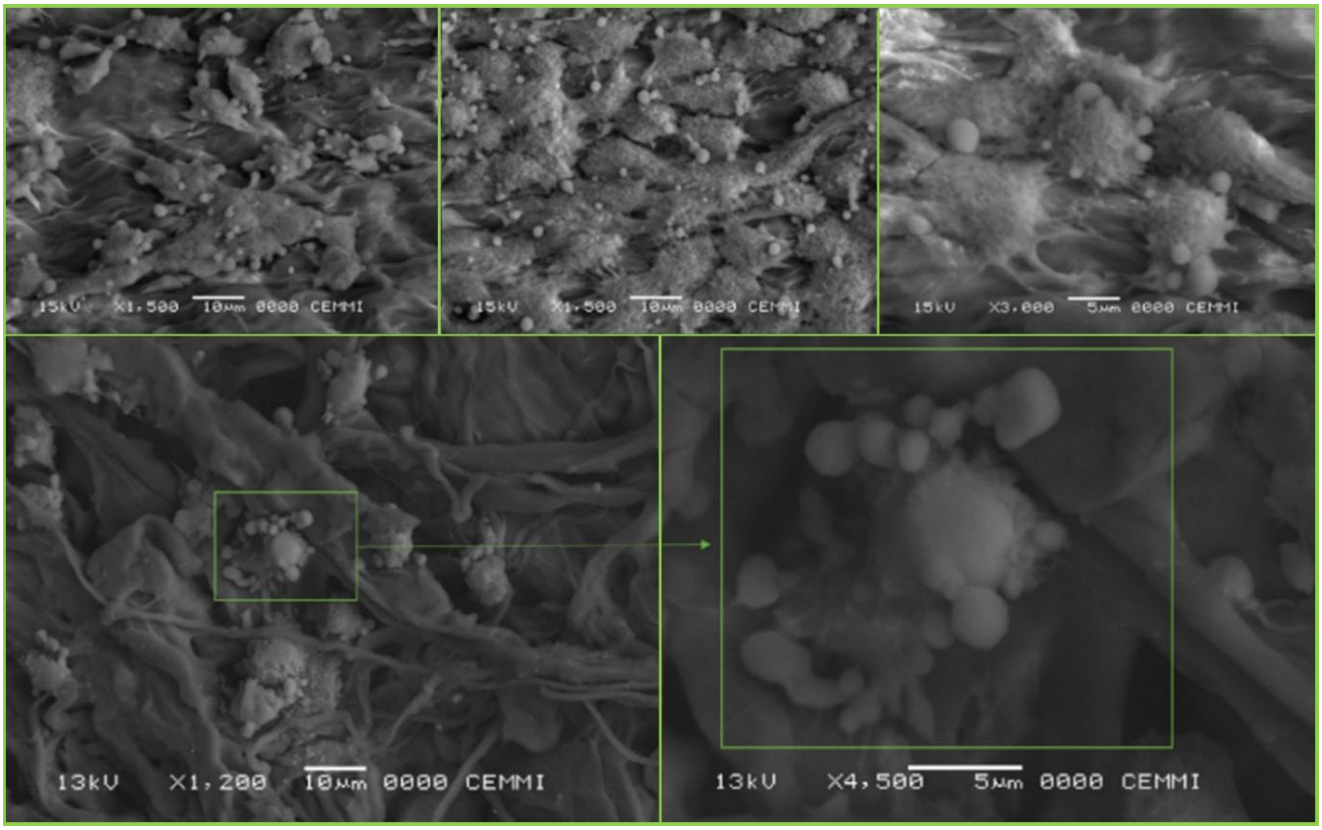


Figure 7. Scanning electron micrographs of SaOS-2 osteoblast-like cells attaching to the surface of the Jason membrane (Straumann Holding AG., Basel, Switzerland), exhibiting visible bleb development on their plasma membrane. The cells have an expanded morphology, with many cytoplasmic extensions and plainly visible blebs, indicating active cell–material interaction.

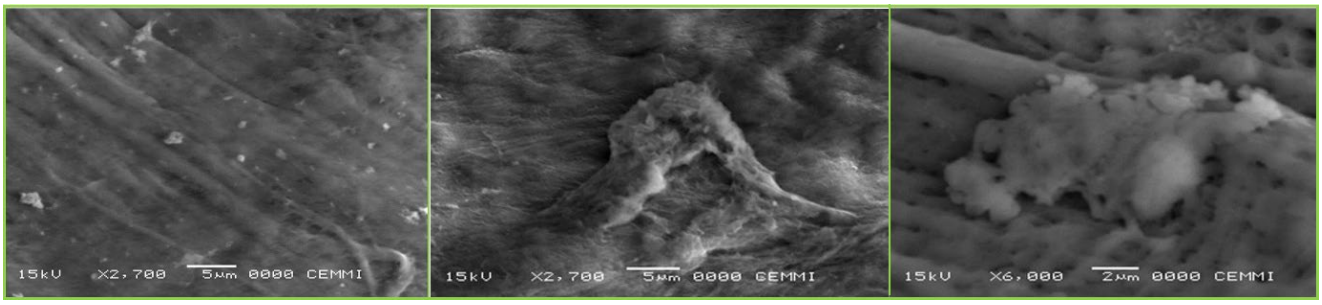


Figure 8. Scanning electron micrographs of SaOS-2 osteoblast-like cells attaching to the surface of the Quirumatrix membrane (Cells Tech Co., Medellín, Colombia). Compared with cells on the Jason membrane (Straumann Holding AG., Basel, Switzerland), the Quirumatrix cells have a more triangular morphology, defined borders, and fewer cytoplasmic extensions. The membrane has a decreased cell density, indicating less proliferation under these conditions.

lated variability inherent to primary cultures, enabling rigorous comparative assessment under controlled conditions [15]. Nevertheless, it must be acknowledged that SaOS-2 cells exhibit altered proliferative kinetics compared to primary osteoblasts and do not fully replicate the cellular heterogeneity or complex signaling networks present during *in vivo* tissue regeneration [16]. Therefore, while these findings provide valuable prelim-

https://doi.org/10.5395/rde.2026.51.e20

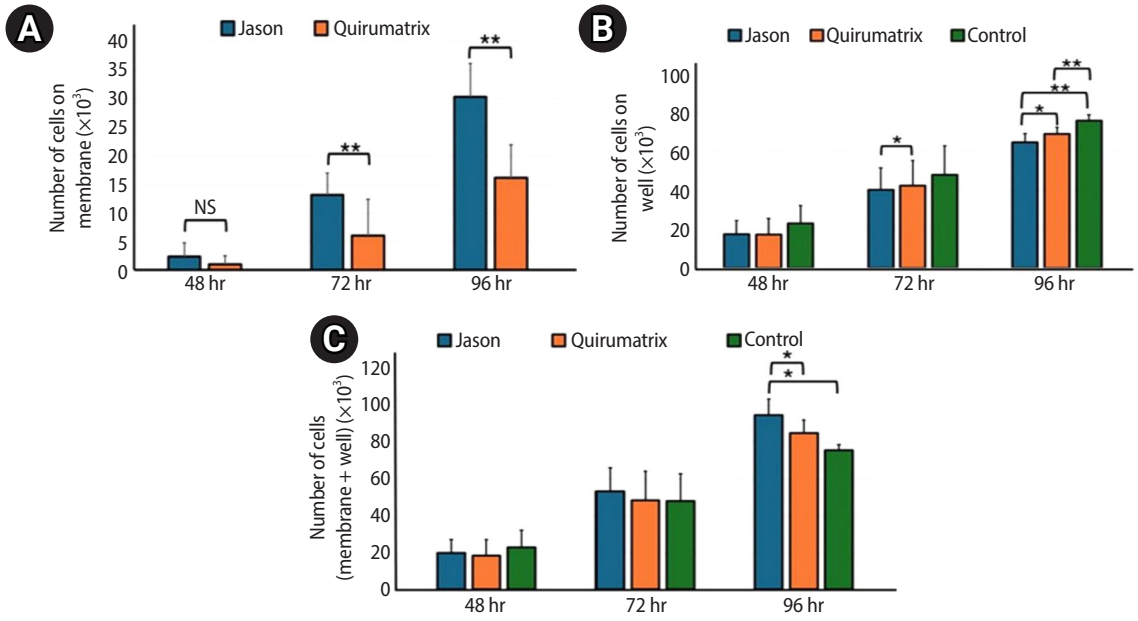


Figure 9. Viability and proliferation of SaOS-2 cells adhered on (A) membrane, (B) well, and (C) total number of cells (well + membrane) at different times (48, 72, and 96 hours). The control group corresponds to cells seeded directly in the well without the presence of the membrane (*$p < 0.05$, **$p < 0.01$). Data are expressed as averages ± standard deviation ($n = 9$). NS, not significant. Jason: Straumann Holding AG., Basel, Switzerland; Quirumatrix: Cells Tech Co., Medellín, Colombia.

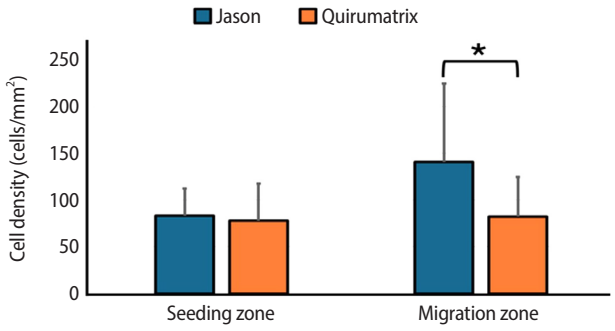


Figure 10. Number of cells/mm^2 counted in the seeding zone and in the cell migration zone of the Jason (Straumann Holding AG., Basel, Switzerland) and Quirumatrix (Cells Tech Co., Medellín, Colombia) membranes after 3 days of culture (*$p < 0.05$). Data are expressed as averages ± standard deviation ($n = 30$).

inary evidence of membrane biocompatibility, future studies incorporating primary cells and *in vivo* models are essential to validate the clinical applicability of these membranes, as discussed in the Study Limitations section.

GTR has been advocated as an adjunct to endodontic surgical procedures to promote complete periapical regeneration by preventing connective tissue collapse within the defect [12]. Barrier membranes are central to this approach, as their shielding function preserves the regenerative space while selectively favoring the repopulation of the defect by periodontal ligament-derived cells and osteogenic precursors [17]. Moreover, semi-permeable membranes contribute to the regulation of the local microenvironment by modulating the diffusion of key biomolecules, including pro-angiogenic growth factors, cytokines, and essential nutrients required for tissue regeneration [8].

Most barrier membranes used in GTR are manufactured from xenogeneic porcine collagen, predominantly type I and/or type III. Native collagen derived from porcine dermis or pericardium has been shown to provide effective barrier function and mechanical stability in regenerative procedures [18]. Beyond its structural role, collagen exhibits chemotactic properties that support fibroblast recruitment and the differentiation, proliferation, and migration of specialized cell populations. Moreover, collagen plays a central role in wound healing, particularly by facilitating platelet activation and angiogenesis [19]. Notably, only in the past decade has

research begun to elucidate the mechanisms governing membrane–host interactions in GTR. Accumulating evidence suggests that barrier membranes may actively contribute to tissue regeneration, as cellular and molecular responses to the membrane surface are intrinsically linked to regenerative outcomes [18,20]. Accordingly, membrane biocompatibility has emerged as a critical determinant of successful tissue regeneration [18].

Decellularized ECM-derived membranes have gained increasing attention as biologically active scaffolds for regenerative applications. The ECM constitutes a complex three-dimensional network composed of structural and signaling macromolecules, including collagen, elastin, fibronectin, laminin, glycosaminoglycans, and proteoglycans, which collectively recapitulate key features of native tissue architecture [21]. Following decellularization, many of the ECM's physicochemical cues and bioactive molecules can be preserved, thereby providing a biologically instructive three-dimensional substrate that supports cell adhesion, migration, proliferation, and differentiation [21]. In addition, ECM-based scaffolds contribute to the maintenance of local tissue homeostasis, facilitate the ingrowth of stem and progenitor cells, and promote regenerative processes through matrix-mediated signaling [21,22]. Accordingly, ECM-derived membranes may offer biologically relevant cues that mimic native signaling events and support the regeneration of damaged periodontal and periapical tissues [21,23].

In this study, a hydration approach was standardized before conducting the biocompatibility assessment of the two membranes to achieve optimal attachment, viability, proliferation, and migration in each membrane. The membranes were hydrated for 48 hours prior to cell seeding using 100% FBS (GE Healthcare Life Sciences, cat. #SH30088.03). This protocol was adopted after preliminary experiments showed that hydration of Quirumatrix membranes in PBS for 24 hours hindered initial cell attachment, with the few adherent cells detaching and undergoing cell death within 12 hours after seeding. One possible explanation for this observation may relate to membrane processing-associated factors inherent to ECM-derived scaffolds. In this context, the potential presence of residual traces of sodium dodecyl sulphate (SDS), an ionic detergent commonly used during decellularization procedures, has been proposed in the literature as a factor that may influence cell–material interactions. Decellularization is performed to minimize adverse host responses, including immune activation, inflammation, and implant rejection, by removing cellular remnants from tissue-derived biomaterials. However, detergents such as SDS are known to denature proteins and alter matrix ultrastructure, and incomplete removal has been associated with cytotoxic effects in some experimental models [24–26]. Importantly, residual SDS content was not directly quantified in the present study; therefore, its potential contribution should be considered hypothetically rather than as a confirmed mechanistic explanation. Notably, FBS has been reported to enhance cell colonization of decellularized tissues [27,28], potentially through protein adsorption and serum-detergent interactions that may facilitate the neutralization or removal of detergent residues [29]. Following optimization of the hydration protocol using 100% FBS, biocompatibility assays were subsequently conducted on both membranes.

Results from this study revealed that both membranes permitted cell attachment, viability, proliferation, and migration, indicating their potential clinical value. Jason outperformed Quirumatrix in terms of biocompatibility. Native collagen in Jason membranes has a robust fibrillar structure, providing exceptional mechanical stability. This natural structure not only provides appropriate strength at the implantation site but also serves as an efficient barrier to epithelial cell invasion, which is necessary for bone and gingival regeneration [30]. This could directly impact its use in patients by enabling faster, more effective regeneration of bone and gingival tissues, thereby improving long-term clinical outcomes [31,32].

Turri *et al.* [33] demonstrated that ECM-based membranes offer significant advantages for guided bone regeneration because their composition is rich in structural proteins, growth factors, and bioactive elements that facilitate cellular integration and the formation of new bone tissue. These membranes release growth factors, including vascular endothelial growth factor and transforming growth factor beta, which promote angiogenesis and bone healing. They attract progenitor cells and stimulate osteoblast differentiation. Its natural

https://doi.org/10.5395/rde.2026.51.e20

structure resembles the human ECM, providing a favorable environment for cell adhesion and proliferation while eliciting no substantial immunological response [33]. The above suggests that Quirumatrix membranes are a promising alternative for GTR; however, the current study's results must be interpreted with caution, although only some aspects of biocompatibility were evaluated. Quirumatrix is an experimental membrane that requires additional studies with more analysis variables. The differences in results between the two membranes could be attributed to a variety of factors, the first of which could be the presence of residual SDS on the Quirumatrix membranes, as previously noted [26,28,29]. Membranes treated with 100% FBS have been shown to increase cellular colonization of decellularized tissues by enriching them with adhesion proteins, growth hormones, and critical nutrients that aid in the early interaction between cells and the substrate [28]. After standardizing appropriate hydration regimens with 100% FBS, biocompatibility testing of both membranes showed that they can be used therapeutically.

Under the parameters of this *in vitro* study, more cells attached to Jason membranes than to Quirumatrix membranes. However, both membranes allowed cell adhesion, which is required for processes such as cell proliferation and migration. This supports other studies suggesting that cells' capacity to adhere to the substrate drives cell proliferation and migration [34]. The attachment of cells to substrates involves a four-step sequence: adsorption of glycoproteins to the substrate surface, cell contact, attachment, and spreading. In general, cell migration and proliferation begin only after these events have occurred. Proper adhesion provides physical anchorage, allowing cells to reorganize their cytoskeleton and extend projections, facilitating their movement toward specific areas of the tissue [35]. This could explain how cells linked to Jason membranes extend and create protrusions known as blebs on their cell membranes. Blebs, which are dynamic protrusions of the plasma membrane driven by intracellular pressure and cytoskeletal remodeling, enable cells to explore their environment and make initial contact with collagen fibers in the ECM. These interactions promote cell adhesion by activating receptors, such as integrins, which bind to collagen's bioactive regions. Furthermore, blebs act as temporary anchoring points for cell migration, generating mechanical forces that propel movement in specific directions [36].

Bleb formation is favored under conditions with low substrate adhesion, a dense or poorly degradable ECM, and high intracellular contractility [37]. Biomaterials used in GTR are typically designed with porous or micro-structured architectures that direct cell migration and proliferation toward the area to be regenerated [38]. However, these structures can represent physically restrictive environments where conventional mesenchymal migration is limited. In this scenario, blebbing-mediated amoeboid migration allows cells to advance without relying on strong adhesion or enzymatic matrix degradation, mechanically adapting to confinement and promoting efficient colonization of the scaffold [37]. This migration modality not only improves cell distribution within the biomaterial but also enhances cell–material interactions and promotes localized secretion of pro-regenerative factors, which are essential for effective tissue repair.

No bleb development was observed in cells adhering to Quirumatrix, unlike on the Jason membrane. This could be due to structural and physical-chemical variations between the two membranes. Jason membranes retain their natural honeycomb-shaped collagen type III structure, characterized by high porosity and multilayered organization. Its porous surface can provide bioactive areas and sufficient mechanical pressure to induce bleb formation, which is required for cell adhesion and migration. On the other hand, the Quirumatrix membrane, while rich in collagen, has a less porous structure, which may limit cell–material interaction and, as a result, bleb formation. These differences highlight the importance of the material's physical and chemical properties in the cellular response, implying that the Jason membrane may provide a more favorable environment for key cellular processes in GTR [38].

It should be noted that, while bleb formation was observed on cells adhering to Jason membranes, the presence of blebs alone does not provide definitive evidence of the cell migration mode. SEM images reveal cell morphology but cannot confirm whether cells are employing amoeboid-like migration or other motility mechanisms. Functional assays, such as live-cell imag-

ing or migration inhibition studies, would be required to determine the actual migration behavior in response to substrate properties. Therefore, the observations presented here should be interpreted as indicative of potential cellular adaptations rather than as conclusive evidence of a specific migration mode.

The decreased number of cells attached to Quirumatrix membranes may also explain the slower pace of cell migration and proliferation compared to the Jason membranes. However, when cell viability was assessed, the total number of cells observed in the membranes and wells was significantly higher in both Jason and Quirumatrix than in the control group, indicating that both membranes significantly stimulated the proliferation of SaOS-2 preosteoblastic cells. Takata *et al*. [35] found that changes in collagen fibril cross-linking, surface roughness, and collagen molecule structure could explain the varying effects on cell adhesion and proliferation. These findings support our SEM observations, which revealed differences in porosity and surface roughness among collagen membranes.

Several limitations of the present *in vitro* investigation should be acknowledged. The biological responses reported herein were derived from the osteoblast-like SaOS-2 cell line, which originates from osteosarcoma and therefore exhibits adhesion, proliferation, and migratory characteristics that may differ from those of primary human osteoblasts, periodontal ligament stem cells, or other progenitor cell populations directly involved in physiological bone and periodontal regeneration. Consequently, the observed cellular behaviors should be interpreted as indicative of relative biocompatibility and cell–material interaction rather than as a direct surrogate for clinical bone regeneration outcomes. In addition, the simplified *in vitro* experimental environment does not fully recapitulate the complex cellular, molecular, and immunological interactions that occur *in vivo*, including inflammatory signaling, vascularization, and multicellular crosstalk. It should be clarified that the terms "biocompatible" and "non-cytotoxic" refer specifically to *in vitro* experimental conditions. While these findings indicate that the material does not adversely affect cell viability under controlled laboratory settings, they do not necessarily predict the *in vivo* biological response, which may be influenced by complex factors such as immune reactions, tissue integration, and long-term material degradation. Therefore, *in vitro* assessments provide initial indications of safety, but further *in vivo* studies are required to fully establish the material's biocompatibility. These limitations underscore the need for complementary studies using primary cells and *in vivo* models to further validate the translational relevance of the present findings.

CONCLUSIONS

Within the constraints of this *in vitro* experimental model, both xenogeneic resorbable membranes exhibited adequate biocompatibility, supporting osteoblast-like cell survival, attachment, and migration. However, clear material-dependent differences in cellular behavior were observed. The Straumann Jason native porcine pericardium collagen membrane demonstrated superior capacity to promote osteoblast-like cell adhesion, proliferation, and directional migration, suggesting a more permissive microenvironment for early osteogenic events.

These findings highlight that membrane performance in GTR extends beyond passive barrier function and is critically influenced by the molecular and structural properties of the biomaterial. Features such as collagen organization, surface topography, and biochemical composition appear to modulate cell–material interactions at the level of cytoskeletal organization, adhesion dynamics, and migratory mechanisms, which are essential determinants of regenerative competence.

Collectively, the results support the concept that barrier membranes actively participate in the regulation of cellular behavior during the early phases of tissue regeneration. While the Quirumatrix ECM-derived membrane represents a biologically promising strategy, its regenerative performance appears to be highly sensitive to processing-related factors that may influence matrix integrity and cell-substrate signaling. Further mechanistic and translational studies are therefore required to elucidate how material-driven molecular cues modulate host cell responses and to define their clinical relevance in regenerative endodontic and periodontal applications.

https://doi.org/10.5395/rde.2026.51.e20

CONFLICT OF INTEREST

No potential conflict of interest relevant to this article was reported.

ACKNOWLEDGMENTS

The authors would like to thank Dr. Lina Escobar, Dr. Zita Bendahan, and Dr. Jaime Castellanos from Universidad del Bosque for their valuable expertise in the execution of this project.

AUTHOR CONTRIBUTIONS

Conceptualization, Visualization: Fernández-Grisales R, Berruecos-Orozco C. Data curation: Fernández-Grisales R, Berruecos-Orozco C, Duque VE, Serna-Guisao D. Formal analysis, Investigation: Fernández-Grisales R, Berruecos-Orozco C, Duque VE, Serna-Guisao D, Rojas WJ, Ríos-Osorio N. Methodology, Software: Duque VE, Serna-Guisao D. Project administration: Fernández-Grisales R. Resources: Ríos-Osorio N. Supervision: Fernández-Grisales R, Berruecos-Orozco C, Calle-Jaramillo M, Rojas WJ. Validation: Fernández-Grisales R, Berruecos-Orozco C, Ríos-Osorio N. Writing - original draft: Ríos-Osorio N. Writing - review & editing: Fernández-Grisales R, Berruecos-Orozco C, Ríos-Osorio N. All authors read and approved the final manuscript.

DATA SHARING STATEMENT

The datasets are not publicly available but are available from the corresponding author upon reasonable request.

REFERENCES

1. Liu TJ, Zhou JN, Guo LH. Impact of different regenerative techniques and materials on the healing outcome of endodontic surgery: a systematic review and meta-analysis. Int Endod J 2021;54:536-555.
2. Rios Osorio N, Caviedes-Bucheli J, Mosquera-Guevara L, Adames-Martinez JS, Gomez-Pinto D, Jimenez-Jimenez K, *et al*. The paradigm of the inflammatory radicular cyst: biological aspects to be considered. Eur Endod J 2023;8:20-36.
3. Lin L, Chen MY, Ricucci D, Rosenberg PA. Guided tissue regeneration in periapical surgery. J Endod 2010;36:618-625.
4. Melcher AH. On the repair potential of periodontal tissues. J Periodontol 1976;47:256-260.
5. Karamifar K, Tondari A, Saghiri MA. Endodontic periapical lesion: an overview on the etiology, diagnosis and current treatment modalities. Eur Endod J 2020;5:54-67.
6. Deng Y, Zhu X, Yang J, Jiang H, Yan P. The effect of regeneration techniques on periapical surgery with different protocols for different lesion types: a meta-analysis. J Oral Maxillofac Surg 2016;74:239-246.
7. Alkandari FA, Alotaibi MK, Al-Qahtani S, Alajmi S. The use of guided tissue regeneration in endodontic microsurgery: setting a threshold. Saudi Dent J 2024;36:461-465.
8. Bashutski JD, Wang HL. Periodontal and endodontic regeneration. J Endod 2009;35:321-328.
9. Yoo CK, Jeon JY, Kim YJ, Kim SG, Hwang KG. Cell attachment and proliferation of osteoblast-like MG63 cells on silk fibroin membrane for guided bone regeneration. Maxillofac Plast Reconstr Surg 2016;38:17.
10. Wang HL, Miyauchi M, Takata T. Initial attachment of osteoblasts to various guided bone regeneration membranes: an in vitro study. J Periodontal Res 2002;37:340-344.
11. Takata T, Wang HL, Miyauchi M. Migration of osteoblastic cells on various guided bone regeneration membranes. Clin Oral Implants Res 2001;12:332-338.
12. Anoopkumar-Dukie S, Carey JB, Conere T, O'sullivan E, van Pelt FN, Allshire A. Resazurin assay of radiation response in cultured cells. Br J Radiol 2005;78:945-947.
13. Czekanska EM, Stoddart MJ, Richards RG, Hayes JS. In search of an osteoblast cell model for in vitro research. Eur Cell Mater 2012;24:1-17.
14. Rodan SB, Imai Y, Thiede MA, Wesolowski G, Thompson D, Bar-Shavit Z, *et al*. Characterization of a human osteosarcoma cell line (Saos-2) with osteoblastic properties. Cancer Res 1987;47:4961-4966.
15. Declercq H, Van den Vreken N, De Maeyer E, Verbeeck R, Schacht E, De Ridder L, *et al*. Isolation, proliferation and differentiation of osteoblastic cells to study cell/biomaterial interactions: comparison of different isolation techniques and source. Biomaterials 2004;25:757-768.
16. Pautke C, Schieker M, Tischer T, Kolk A, Neth P, Mutschler W, *et al*. Characterization of osteosarcoma cell lines MG-63, Saos-2 and U-2 OS in comparison to human osteoblasts. Anticancer Res 2004;24:3743-3748.
17. Zubizarreta-Macho Á, Tosin R, Tosin F, Velasco Bohórquez P, San Hipólito Marín L, Montiel-Company JM, *et al*. Influence of guided tissue regeneration techniques on the success rate of healing of surgical endodontic treatment: a systematic review and network meta-analysis. J Clin Med 2022;11:1062.
18. Sasaki JI, Abe GL, Li A, Thongthai P, Tsuboi R, Kohno T, *et al*. Barrier membranes for tissue regeneration in dentistry. Biomater Investig Dent 2021;8:54-63.
19. Lindner C, Alkildani S, Stojanovic S, Najman S, Jung O, Barbeck M. In vivo biocompatibility analysis of a novel barrier membrane based on bovine dermis-derived collagen for

Guided Bone Regeneration (GBR). Membranes (Basel) 2022;12:378.
20. Alqahtani AM, Moorehead R, Asencio IO. Guided tissue and bone regeneration membranes: a review of biomaterials and techniques for periodontal treatments. Polymers (Basel) 2023;15:3355.
21. Omar O, Elgali I, Dahlin C, Thomsen P. Barrier membranes: more than the barrier effect? J Clin Periodontol 2019;46 Suppl 21(Suppl Suppl 21):103-123.
22. Liang C, Liao L, Tian W. Advances focusing on the application of decellularized extracellular matrix in periodontal regeneration. Biomolecules 2023;13:673.
23. Liu C, Pei M, Li Q, Zhang Y. Decellularized extracellular matrix mediates tissue construction and regeneration. Front Med 2022;16:56-82.
24. Mendibil U, Ruiz-Hernandez R, Retegi-Carrion S, Garcia-Urquia N, Olalde-Graells B, Abarrategi A. Tissue-specific decellularization methods: rationale and strategies to achieve regenerative compounds. Int J Mol Sci 2020;21:5447.
25. Alizadeh M, Rezakhani L, Soleimannejad M, Sharifi E, Anjomshoa M, Alizadeh A. Evaluation of vacuum washing in the removal of SDS from decellularized bovine pericardium: method and device description. Heliyon 2019;5:e02253.
26. Gratzer PF, Harrison RD, Woods T. Matrix alteration and not residual sodium dodecyl sulfate cytotoxicity affects the cellular repopulation of a decellularized matrix. Tissue Eng 2006;12:2975-2983.
27. Long C, Galvez MG, Legrand A, Joubert LM, Wang Z, Chattopadhyay A, *et al*. Intratendinous injection of hydrogel for reseeding decellularized human flexor tendons. Plast Reconstr Surg 2017;139:1305e-1314e.
28. Porzionato A, Stocco E, Barbon S, Grandi F, Macchi V, De Caro R. Tissue-engineered grafts from human decellularized extracellular matrices: a systematic review and future perspectives. Int J Mol Sci 2018;19:4117.
29. Jafari M, Mehrnejad F, Rahimi F, Asghari SM. The molecular basis of the sodium dodecyl sulfate effect on human ubiquitin structure: a molecular dynamics simulation study. Sci Rep 2018;8:2150.
30. Cho YD, Kim KH, Lee YM, Ku Y, Seol YJ. Periodontal wound healing and tissue regeneration: a narrative review. Pharmaceuticals (Basel) 2021;14:456.
31. Opris H, Baciut M, Moldovan M, Cuc S, Petean I, Opris D, *et al*. Comparison of the eggshell and the porcine pericardium membranes for guided tissue regeneration applications. Biomedicines 2023;11:2529.
32. Sbricoli L, Guazzo R, Annunziata M, Gobbato L, Bressan E, Nastri L. Selection of collagen membranes for bone regeneration: a literature review. Materials (Basel) 2020;13:786.
33. Turri A, Elgali I, Vazirisani F, Johansson A, Emanuelsson L, Dahlin C, *et al*. Guided bone regeneration is promoted by the molecular events in the membrane compartment. Biomaterials 2016;84:167-183.
34. Merino-Casallo F, Gomez-Benito MJ, Hervas-Raluy S, Garcia-Aznar JM. Unravelling cell migration: defining movement from the cell surface. Cell Adh Migr 2022;16:25-64.
35. Takata T, Wang HL, Miyauchi M. Attachment, proliferation and differentiation of periodontal ligament cells on various guided tissue regeneration membranes. J Periodontal Res 2001;36:322-327.
36. Paluch EK, Raz E. The role and regulation of blebs in cell migration. Curr Opin Cell Biol 2013;25:582-590.
37. Schick J, Raz E. Blebs-formation, regulation, positioning, and role in amoeboid cell migration. Front Cell Dev Biol 2022;10:926394.
38. Ren Y, Fan L, Alkildani S, Liu L, Emmert S, Najman S, *et al*. Barrier membranes for guided bone regeneration (GBR): a focus on recent advances in collagen membranes. Int J Mol Sci 2022;23:14987.

https://doi.org/10.5395/rde.2026.51.e20